Sensorless Control of Wound Rotor Synchronous Motors Based on Rotor High-Frequency Signal Injection

David Reigosa, Ye Gu Kang, María Martínez, Daniel Fernández, J. M. Guerrero and Fernando Briz
University of Oviedo. Dept. of Elect., Computer & System Engineering, Gijón, 33204, Spain.
diazdavid@uniovi.es, kangye@uniovi.es, martinezgmaria@uniovi.es, fernandezalodaniel@uniovi.es,
guerrero@uniovi.es, fernando@isa.uniovi.es

Abstract: High frequency (HF) signal injection-based methods have been widely investigated for sensorless position/speed control of permanent magnet synchronous machines (PMSMs). In PMSMs, the HF signal must be injected in the stator windings and an asymmetric (salient) rotor is required. Contrary to this, both stator and rotor terminals are accessible in wound-rotor synchronous motors (WRSMs). It is feasible therefore to inject the HF signal in the rotor, and, as a consequence, the method will not rely on the rotor asymmetry.[1]

Keywords—Wound rotor synchronous machines, sensorless control, high frequency signal injection.

I. Introduction

Permanent Magnet Synchronous Motors (PMSMs) have been the preferred option for electric and hybrid-electric vehicles (EV & HEV) due to their high torque density, wide speed capability and higher efficiency compared with other machine types like DC or induction machines (IM's). Wound-rotor synchronous motors (WRSMs) can be an alternative to PMSMs in EV & HEV [1]-[2], they have been successfully used in Renault Zoé, Fluence and Kangoo EVs[1].

Sensorless control of the traction electric motor in EV & HEV is highly appealing as it results in a reliability increase and a cost reduction thanks to the elimination of the position/speed sensor, cabling and connectors. While a large amount of work has been published on the sensorless control of PMSM's and IM's [3]-[16], much less attention has been paid to the case of WRSMs [1], [17]-[20].

Sensorless methods can be roughly classified into fundamental excitation-based methods and HF signal injection-based methods. Fundamental excitation-based methods can be considered a mature field, and are available in many electric drives. These methods operate well in the mid-high speed region where the back-EMF signal is large enough. However, their accuracy reduces with speed. Consequently, they cannot work at very low or zero speed, do not allow position control either [4]-[5]. To overcome the limitations of the fundamental excitation-based methods in the low speed region, HF signal injection based methods were proposed. When used with IMs and PMSMs [3]-[12], the HF signal is injected into the stator terminals via inverter. Both the use of the PWM commutations [7], as well as the injection of a periodic HF signal on top the fundamental excitation have been proposed for this purpose. Waveshapes for the HF signal include rotating [3], [8]-[11], pulsating [8]-[11] and square-wave [12].

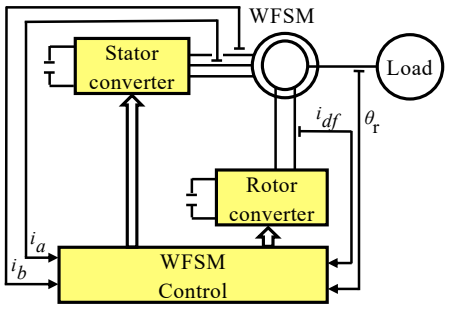

Fig. 1.-. Simplified energy conversion system of WRSM

A key issue for the implementation of HF signal injection methods in machines for which only the stator is accessible (IMs, PMSMs, synchronous reluctance machines) is that the rotor must be salient. Rotor position is obtained by processing of the resulting HF currents which result from the interaction between the injected HF voltage and the rotor saliencies.

In a WRSM, both stator and rotor terminals are available (see Fig. 1) what opens new possibilities for the implementation of HF signal injection-based sensorless methods compared to other types of three-phase AC machines with the exception of DFIG [21]. HF signal injection sensorless control techniques have been recently extended to WRSM [1], [17]-[20]. In [1], [17] and [19], the HF signal is injected in the stator terminals, while injection in the rotor terminals was proposed in [18]-[20]. In all the cases the injected HF signal was a voltage. The estimated position will depend in this case on the machine HF impedance, which will vary due to saturation.

In the method proposed in this paper, a HF current is injected in the rotor via rotor side power converter. Both the induced stator current and voltage will be shown to contain an HF component modulated by the rotor angle. Two different implementations will be analyzed in this paper: 1) using the

[1] This work was supported in part by the Research, Technological Development and Innovation Programs of the Spanish Ministry Economy and Competitiveness, under grant MINECO-17-ENE2016-80047-R and by the Government of Asturias under project IDI/2018/000188 and FEDER funds.

induced stator HF current; 2) using the stator HF voltage with the stator HF current being cancelled. It will be shown that option 2) reduces the losses due to HF signal injection and is insensitive the stator HF impedance [22]; this will be at the price of a slight increase of the implementation complexity difficulties. In both cases the estimation is not affected by the rotor field winding impedance.

The paper is organized as follow: the fundamental and HF models of a WRSM are presented in Section II; physical principles of the method are presented in Section III; simulation results to confirm the viability of the method are provided in Section IV, conclusions being provided in Section VI.

II. WRSM model

The fundamental model of a WRSM in a synchronous frame with the *d*-axis being aligned with the field winding is given by (1)-(3) [23], where R_d, R_q, L_d and L_q are the *d* and *q-axes* resistances and inductances respectively, L_{mq} is the *d*-axis mutual inductance, L_f is the field winding inductance, N_s is the stator number of turns, N_{fd} is the field winding number of turns, v^r_{sd} and v^r_{sq} are the *d*- and *q*-axes stator voltages, i^r_{sd} and i^r_{sq} are the *d*- and *q*-axes stator currents, i_{fd} is the field winding current, v_{fd} is the field winding voltage and ω_r is the rotor speed. Primed variables in (4), (5), (6) and (7) are referred to the stator.

$$v^r_{sd}=R_d i^r_{sd}+L_d\frac{di^r_{sd}}{dt}+L_{md}\frac{di^{'}_{fd}}{dt}-\omega_r L_q i^r_{sq} \quad (1)$$

$$v^r_{sq}=R_q i^r_{sq}+L_q\frac{di^r_{sq}}{dt}+\omega_r L_d i^r_{sd}+\omega_r L_{md} i^{'}_{fd} \quad (2)$$

$$v^{'}_{fd}=R^{'}_f i^{'}_{fd}+L^{'}_f\frac{di^{'}_{fd}}{dt}+L_{md}\frac{di^r_{sd}}{dt} \quad (3)$$

$$R^{'}_f=\left(N_s/N_{fd}\right)^2 R_f \quad (4)$$

$$L^{'}_f=\left(N_s/N_{fd}\right)^2 L_f \quad (5)$$

$$i^{'}_{fd}=\left(N_{fd}/N_s\right) i_{fd} \quad (6)$$

$$v^{'}_{fd}=\left(N_s/N_{fd}\right) v_{fd} \quad (7)$$

If the WRSM is fed with a signal with a frequency sufficiently larger than the fundamental frequency., rotor speed dependent terms and resistive term can be neglected , the HF model in (8)-(10) being obtained from (1)-(3), where subscript "HF" stands for HF variables.

$$v^r_{sdHF}=L_{dHF}\frac{di^r_{sdHF}}{dt}+L_{mdHF}\frac{di^{'}_{fdHF}}{dt} \quad (8)$$

$$v^r_{sqHF}=L_{qHF}\frac{di^r_{sqHF}}{dt} \quad (9)$$

$$v^{'}_{fdHF}=L^{'}_{fHF}\frac{di^{'}_{fdHF}}{dt}+L_{mdHF}\frac{di^r_{sdHF}}{dt} \quad (10)$$

III. HF signal injection and rotor position estimation

Two different implementations are discussed following. In both cases a sinusoidal HF current signal (11) of magnitude I_{HF} and frequency ω_{HF} injected in the rotor using a resonant controller [24]-[25].

$$i_{fdHF}=I_{HF}\sin(\omega_{HF}t) \quad (11)$$

In the first implementation, the HF current induced in the stator is left to flow freely. In the second it is cancelled by means of a HF current controller.

a) <u>Rotor HF current injection without stator HF current cancellation</u>

Injecting (11) in the field winding the resulting stator HF currents (12)-(13) are obtained by making $v^r_{sdHF}=v^r_{sqHF}=0$ in (11)-(12), since the stator inverter does not apply any voltage at this frequency.

$$i^r_{sdHF}=-\frac{L_{mdHF}}{L_{dHF}}i^{'}_{fdHF}=-\frac{L_{mdHF}}{L_{dHF}}\frac{N_{fd}}{N_s}\ i_{fd}=$$
$$=-\frac{L_{mdHF}}{L_{dHF}}\frac{N_{fd}}{N_s}I_{HF}\sin(\omega_{HF}t)=-I^r_{sdHF}\sin(\omega_{HF}t) \quad (12)$$

$$i^r_{sqHF}=0 \quad (13)$$

The stator HF current complex vector i^r_{sdqHF} (14) resulting from (12)-(13) can be decomposed into positive sequence ($i^r_{sdqHFpc}$) and negative sequence ($i^r_{sdqHFnc}$) vectors, each of magnitude half of the original scalar signal. Since the stator current is measured by sensors which are in a stationary reference frame, it is useful to express (14) in the stator reference frame, (15) being obtained.

$$i^r_{sdqHF}=\begin{bmatrix}i^r_{sdHF}\\ i^r_{sqHF}\end{bmatrix}=\begin{bmatrix}-I^r_{sdHF}\sin(\omega_{HF}t)\\ 0\end{bmatrix}=$$
$$=\frac{\left|i^r_{sdqHF}\right|}{2}\left(e^{j(+\omega_{HF}t+\pi/2)}+e^{j(-\omega_{HF}t-\pi/2)}\right)=i^r_{sdqHFpc}+i^r_{sdqHFnc} \quad (14)$$

$$i^s_{sdqHF}=\frac{\left|i^r_{sdqHF}\right|}{2}\left(e^{j(\omega_{HF}t+\pi/2+\theta_r)}+e^{j(-\omega_{HF}t-\pi/2+\theta_r)}\right)=$$
$$=i^s_{sdqHFpc}+i^s_{sdqHFnc} \quad (15)$$

It is observed that the rotor angle, θ_r, is modulated in both the positive sequence $i^s_{sdqHFpc}$ and negative sequence $i^s_{sdqHFnc}$ components forming i^s_{sdqHF}. The rotor position can be therefore obtained by processing the positive or negative sequence component of the HF stator current indistinctly.

Fig. 2a shows the implementation of WRSM sensorless control, including fundamental current control, HF current injection and signal processing to estimate the rotor position. A resonant controller "RES" is used to inject the HF current [24]-[25]. The stator current complex vector is transformed to the estimated rotor reference frame, i^r_{sdq}. This current is used both to feedback the fundamental as well as the input to the speed estimation block. The speed estimation block transforms the current into a reference frame synchronous with the positive sequence component of the injected HF current (16); the rotor speed is obtained by driving the *q*-axis component of the positive sequence of the HF current [see (16)] to zero. The rotor position is obtained by integrating the speed estimate. The speed estimation block diagram is equivalent to a synchronous reference frame phase-lock loop (SRF-PLL) [28].

$$i^{HF}_{sdqHF}=\frac{\left|i^r_{sdqHF}\right|}{2}\left(e^{j(+\pi/2)}+e^{j(-2*\omega_{HF}t-\pi/2)}\right) \quad (16)$$

The implementation in Fig. 2a has some drawbacks:

- It can be observed from (11)-(13) that HF current will flow both through stator and rotor windings, therefore producing losses in both sides. Losses due to HF signal

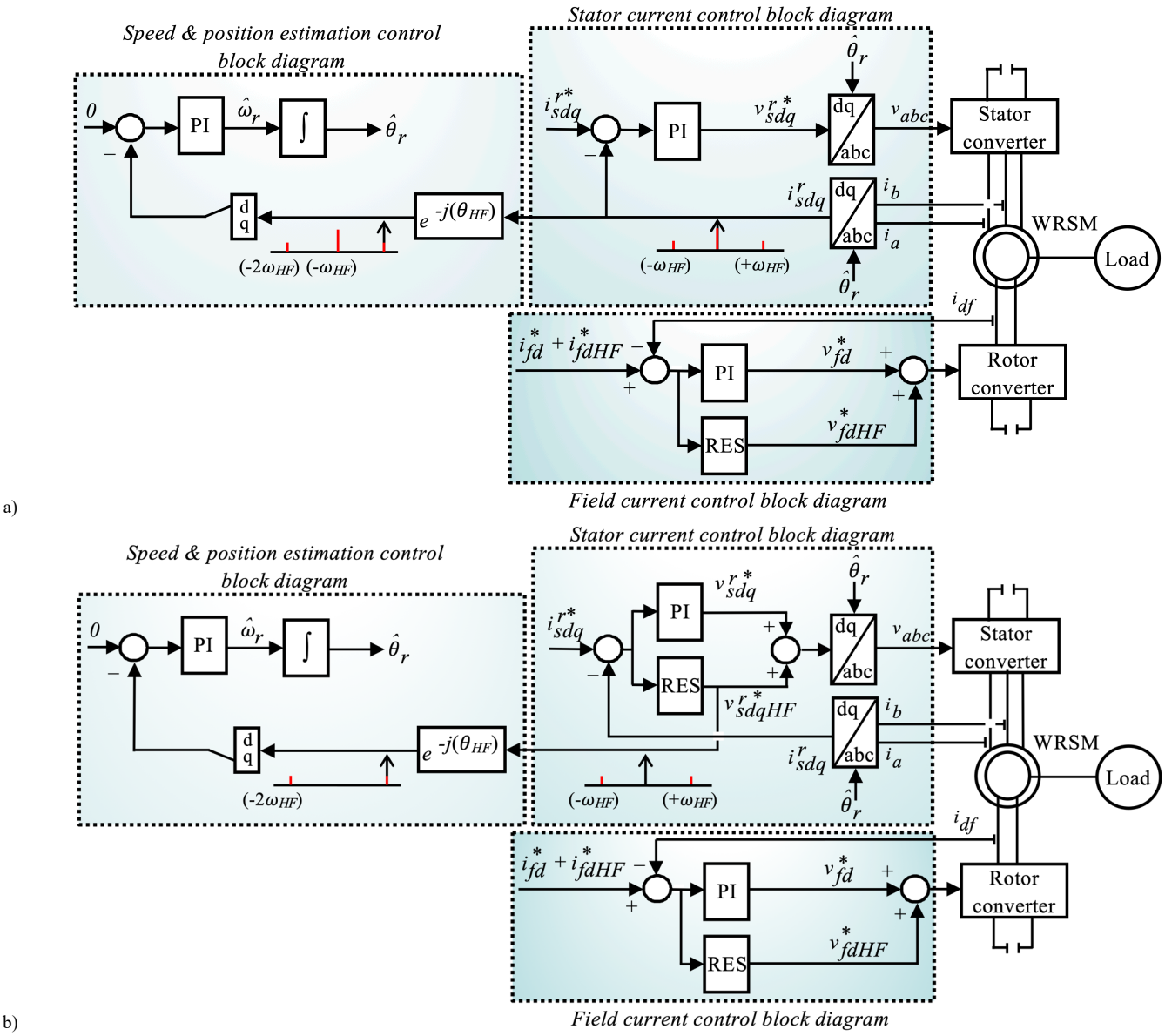

Fig. 2.-. Block diagram of a WRSM including fundamental control, HF signal injection and signal processing using rotor HF current injection a) without and b) with stator HF current cancellation.

injection $P_{HF\ loss}$ can be expressed as (17). Considering only copper and iron eddy current losses, stator and rotor losses will be given by (18) and (19), where $k_{FE\ stator}$ and $K_{FE\ rotor}$ are constants and $B_{HF\ stator}$ and $B_{HF\ rotor}$ are the flux density peak values due to the HF current injection [26]-[27]. Note that (17)-(18) don't include hysteresis losses.

$$P_{HF\ losss}=P_{HF\ stator}+P_{HF\ rotor} \quad (17)$$

$$P_{HF\ stator}=R_{dHF}\left(\frac{I^r_{sdHF}}{\sqrt{2}}\right)^2+k_{FE\ stator}\,(\omega_{HF}B_{HF\ stator})^2 \quad (18)$$

$$P_{HF\ rotor}=R_{fHF}\left(\frac{I_{HF}}{\sqrt{2}}\right)^2+k_{FE\ rotor}\,(\omega_{HF}B_{HF\ rotor})^2 \quad (19)$$

- Torque ripple will be induced due to HF signal injection. Overall output torque of a WRSM is represented by (20) [23], while torque ripple due to the HF signal injection can be expressed as (21), where P is the number of poles. It can be observed that torque ripple results from the interaction among i^r_{sq}, i^r_{sdHF} and $i^{'r}_{fdHF}$, i.e. load current, stator d-axis HF current and field HF current respectively.

$$T_{out}=\frac{3}{2}\frac{P}{2}\left[(L_d-L_q)i^r_{sd}i^r_{sq}+L_{md}i^{'}_{fd}i^r_{sq}\right] \quad (20)$$

$$T_{rippleHF}=\frac{3}{2}\frac{P}{2}\left[(L_d-L_q)i^r_{sdHF}i^r_{sq}+L_{md}i^{'}_{fdHF}i^r_{sq}\right] \quad (21)$$

Aforementioned drawbacks can be improved by implementing HF current cancellation, this is described in the next subsection.

b) Rotor HF current injection with stator HF current cancellation

Assumed that the HF current (11) is injected in the rotor terminals, the condition to cancel the HF current in the stator terminals can be deduced from (8)-(9), i.e. the voltage defined by (21)-(22) must be applied to the stator windings. Use of

(21)-(22) would rely on the accuracy of the machine parameters estimates, a more reliable approach is to use a HF current regulator in the stator converter to make zero the HF component of stator windings current [24]-[25].

$$v^r_{sdHF}=L_{mdHF}\frac{di'_{fdHF}}{dt}=\frac{N_{fd}}{N_s}L_{mdHF}\frac{di_{fdHF}}{dt}= \quad (22)$$
$$=\frac{N_{fd}}{N_s}L_{mdHF}\omega_{HF}I_{HF}\cos(\omega_{HF}t)=V^r_{sdHF}\cos(\omega_{HF}t)$$

$$v^r_{sqHF}=0 \quad (23)$$

The rotor position information will now be modulated in the HF output voltage, i.e. the output of the HF current controller. The HF voltage can be modeled following the same procedure used for the HF current in the previous section. The stator HF voltage complex vector in a reference frame synchronous with the rotor v^r_{sdqHF} (24), can be obtained from (22)-(23), $v^r_{sdqHFpc}$ and $v^r_{sdqHFnc}$ being the positive and negative sequence vector components. v^s_{sdqHF} is the stator HF voltage complex vector in the stator reference frame (25). It is seen from (25) that it is possible to estimate the rotor position θ_r from either the positive or negative sequence components ($v^s_{sdqHFpc}$ and $v^s_{sdqHFnc}$) of v^s_{sdqHF}.

$$v^r_{sdqHF}=\begin{bmatrix}v^r_{sdHF}\\ v^r_{sqHF}\end{bmatrix}=\begin{bmatrix}V^r_{sdHF}\cos(\omega_{HF}t)\\ 0\end{bmatrix}= \quad (24)$$
$$=\frac{|v^r_{sdqHF}|}{2}\left(e^{j(+\omega_{HF}t)}+e^{j(-\omega_{HF}t)}\right)=v^r_{sdqHFpc}+v^r_{sdqHFnc}$$

$$v^s_{sdqHF}=\frac{|v^r_{sdqHF}|}{2}\left(e^{j(\omega_{HF}t+\theta_r)}+e^{j(-\omega_{HF}t+\theta_r)}\right)= \quad (25)$$
$$=v^s_{sdqHFpc}+v^s_{sdqHFnc}$$

Fig. 2b shows the corresponding control block scheme. Two resonant controllers ("RES" blocks) are needed now. The first one is responsible of HF current injection in the field winding, while the second is aimed to force the stator HF current to be zero [24]-[25]. Speed and position are estimated as described in Section IVa.

Compared to the implementation without stator HF current cancellation, this option has a slightly higher complexity as it requires two HF current controllers, but brings two clear advantages:

- Induced losses due to HF signal injection are reduced as now the HF current only flows through the field winding, modification of (16)-(18) for this case being straightforward.
- Since no HF current flows through the stator windings, torque ripple is reduced as now it only results from the interaction between i^r_{sq} and i'_{fdHF} (26).

$$T_{ripple}=\frac{3}{2}\frac{P}{2}\left[L_{md}i'_{fdHF}i^r_{sq}\right] \quad (26)$$

IV. Simulation results

TABLE I MACHINE PARAMETERS

U_{RATED} (V)	I_{RATED} (A)	f_{RATED} (Hz)	P_{RATED} (kW)	ω_{RATED} (rpm)
380	17.5	50	8.1	1500

R_d (Ω)	L_d (H)	L_q (H)	L_{md} (H)	R_f (Ω)	Lf_d (H)
1.62	0.113	0.056	0.108	1.208	0.12

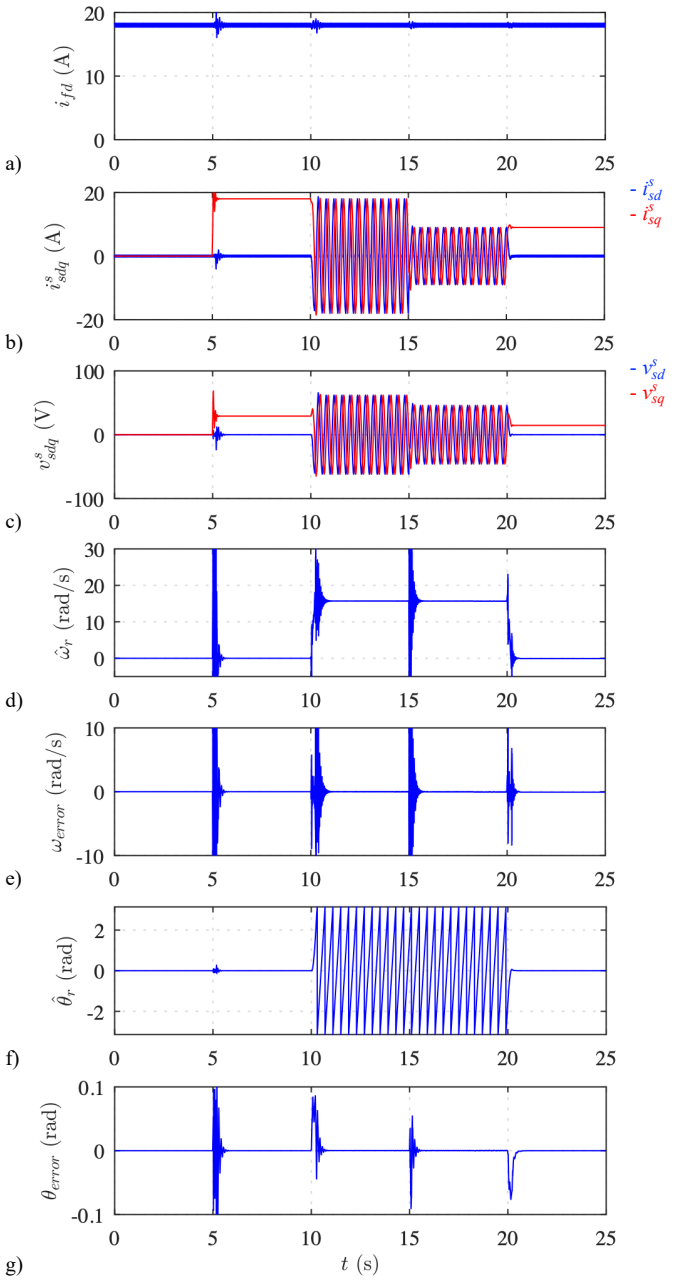

Fig. 3.-. Simulation results for "Rotor HF current injection without stator HF current cancellation". a) field winding current, b) stator *dq*-axis currents, c) Stator *dq*-axis voltage commands, d) estimated speed, e) speed estimation error, f) estimated position and g) position estimation error. ω_{HF}=2·π·500 rad/s, I_{HF}=0.05pu.

This section shows simulation results of the two implementations being considered. Table I shows the parameters of the simulated machine.

a) Rotor HF current injection without stator HF current cancellation

Fig. 3 shows simulation results for the process describe following:

- t=0-5s: I^r_{sq}= 0pu and ω_r=0pu
- t=5s: I^r_{sq} step-like variation from 0 to 1pu (i.e. 17.5A) ; ω_r = 0pu

- t=10 - 10.2s: a ω_r ramp-like variation from 0 to 0.05 pu; I_{sq}^r = 1pu
- t=15s: I_{sq}^r step-like variation from 1 to 0.5pu ; ω_r = 1pu
  t=20 - 20.2s: ω_r ramp-like variation from 1 to 0.0 pu; I_{sq}^r = 0.05pu.

Fig. 3a shows the field winding current consisting of the fundamental field current (i.e. DC) and the HF current. Fig. 3b shows the stator *dq*-axis currents, which is also seen to consists of the AC fundamental current and the induced HF current. Fig. 3c shows the stator *dq*-axis voltages commands, which in this case consist only on the fundamental voltage, i.e. do not include any HF component. Fig. 3d shows the estimated speed, while Fig. 3e shows the speed estimation error. Fig. 3f shows the estimated position, while Fig. 3g shows and the position estimation error, which is seen to be <0.01 rad. Peak-to-peak errors in the estimated speed and position for the different operating conditions are summarized in Table II. It can be observed that the speed error is <0.35 rad/s and the position error is <0.016 rad, the error being almost insensitive to load level, rotor speed I_{sq}^r, and ω_r.

TABLE II SIMULATION RESULTS: ROTOR HF CURRENT INJECTION WITHOUT STATOR HF CURRENT CANCELLATION

	ω_r =0.05 pu, I_{sd}^r=0 pu, I_{HF}=0.1 pu, ω_{HF}=2·π·500 rad/s			
	I_{sq}^r (pu)			
	0	0.25	0.5	1
ω_{error} (rad/s) (pk-to-pk)	0.31	0.33	0.34	0.35
θ_{error} (rad) (pk-to-pk)	0.010	0.011	0.012	0.009
	I_{sdq}^r=0 pu, I_{HF}=0.1 pu, ω_{HF}=2·π·500 rad/s			
	ω_r (pu)			
	0	0.05	0.1	
ω_{error} (rad/s) (pk-to-pk)	0.31	0.34	0.33	
θ_{error} (rad) (pk-to-pk)	0.009	0.011	0.010	
	ω_r =0.05 pu, I_{sdq}^r=0pu, ω_{HF}=2·π·500 rad/s			
	I_{HF} (pu)			
	0.05	0.1	0.15	
ω_{error} (rad/s) (pk-to-pk)	0.32	0.35	0.31	
θ_{error} (rad) (pk-to-pk)	0.016	0.012	0.012	

TABLE III SIMULATION RESULTS: ROTOR HF CURRENT INJECTION WITH STATOR HF CURRENT CANCELLATION

	ω_r =0.05 pu, I_{sd}^r=0 pu, I_{HF}=0.1 pu, ω_{HF}=2·π·500 rad/s			
	I_{sq}^r (pu)			
	0	0.25	0.5	1
ω_{error} (rad/s) (pk-to-pk)	0.49	0.51	0.51	0.53
θ_{error} (rad) (pk-to-pk)	0.013	0.012	0.017	0.015
	I_{sdq}^r=0 pu, I_{HF}=0.1 pu, ω_{HF}=2·π·500 rad/s			
	ω_r (pu)			
	0	0.05	0.1	
ω_{error} (rad/s) (pk-to-pk)	0.49	0.48	0.48	
θ_{error} (rad) (pk-to-pk)	0.02	0.019	0.018	

b) Rotor HF current injection with stator HF current cancellation

Fig. 4 shows simulation results for this operating mode under the same working conditions as for the previous case. Control and signal processing are the same as shown in Fig. 2b. It can be observed from Fig. 4b that stator *dq*-axis currents consist in this case only of the AC fundamental current, no HF current being present. It is also observed from Fig. 4c the *dq*-axis voltages consist of the AC fundamental voltage and the resulting HF voltage to cancel the stator HF current. It can be observed from Fig. 4d-g that the steady state speed and position estimation errors are in the same range as in the "Rotor HF current injection without stator HF current cancellation" mode, see Fig. 3.

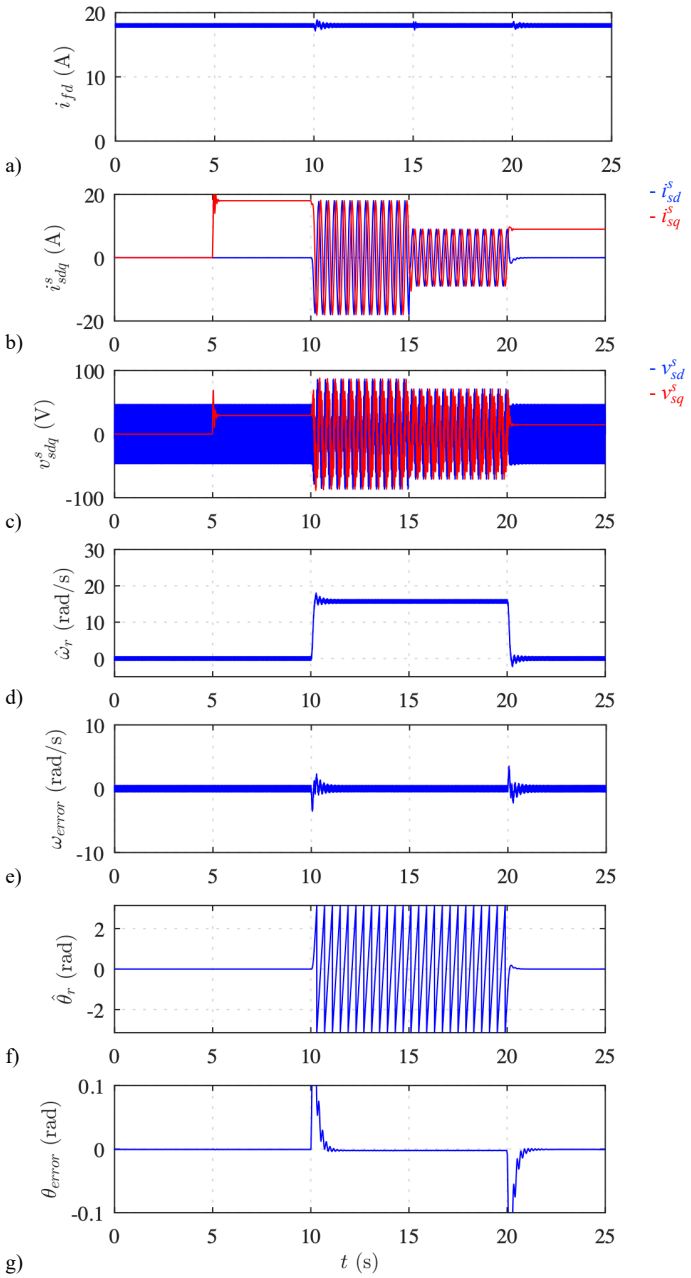

Fig. 4.-. Same simulation results as Fig. 3 but for "Rotor HF current injection with stator HF current cancellation" implementation.

Simulation results for the different scenarios are summarized in Table III. As in the previous implementation, it is observed that the estimated position error is almost independent of I_{sq}^r and ω_r. Both the estimated speed error and estimated position error are observed to be in the same range as when no stator HF current cancellation is applied.

V. Conclusions

This paper proposes the use of HF signal injection for sensorless control of WRSMs. Two different implementations are analyzed. In both cases a HF current is injected in the field winding; either the induced stator HF current or the HF voltage can be used therefore for rotor position estimation. By injecting a injecting a HF current in the field winding the estimation becomes insensitive to the rotor field winding impedance. Implementation based on the induced stator HF voltage has been shown to result in lower induced loss due to HF signal injection, and is also insensitive to the stator HF impedance. This is at the price of a slightly increase of the implementation complexity. Simulation results have been provided to confirm the viability of the proposed methods.

VI. References

[1] M. Koteich, A. Messali and S. Daurelle, "Self-sensing Control of the Externally-Excited Synchronous Machine for Electric Vehicle Traction Application," IEEE Symposium on Sensorless Control of Electric Drives (SLED), pp. 91-96, Sept. 2017

[2] M. Märgner, W. Hackmann, "Control challenges of an externally excited synchronous machine in an automotive traction drive application, " IEEE Emobility - Electrical Power Train Congress, Nov. 2010.

[3] P.L. Jansen and R.D. Lorenz, "Transducerless position and velocity estimation in induction and salient AC machines," IEEE Trans. Ind. Appl., Vol. 31, pp. 240–247, Mar./Apr. 1995.

[4] L. A. de S. Ribeiro, M.C. Harke, and R.D. Lorenz, "Dynamic Properties of Back-emf Based Sensorless Drives," IEEE-IAS, Vol. 4, pp. 2026 - 2033, Oct 2006.

[5] P. P. Acarnely and j. F. Watson, "Review of Position-Sensorless Operation of Brushless Permanent-Magnet Machines," IEEE Trans. Ind. Electron., vol. 53 (2), pp. 352-362, Apr. 2006.

[6] S. Ogasawara and H. Akagi, "Approach to real-time position estimation at zero and low speed for a PM motor based on saliency," IEEE Trans. Ind. Appl., vol. 34, pp. 163-168, Jan.-Feb. 1998.

[7] J. Holtz and H. Pan, "Acquisition of rotor anisotropy signals in sensorless position control systems," IEEE Trans. Ind. Appl. , Sept./Oct. 2004, Vol. 40, No 5, pp. 1379–1387.

[8] P. García, F. Briz, M.W. Degner, D. Díaz-Reigosa, "Accuracy and Bandwidth Limits of Carrier Signal Injection-Based Sensorless Control Methods", IEEE Trans. Ind. Appl., Vol. 43 (4), pp. 990–1001, July/Aug. 2007.

[9] D. Reigosa, P. García, D. Raca, F. Briz, and R.D. Lorenz, "Measurement and Adaptive Decoupling of Cross-Saturation Effects and Secondary Saliencies in Sensorless-Controlled IPM Synchronous Machines," IEEE Trans. Ind. Appl., Vol. 44 (6), pp. 1758–1768, Nov./Dec. 2008.

[10] D. Reigosa, P. García, F. Briz, D. Raca and R.D. Lorenz, "Modeling and adaptive decoupling of transient resistance and temperature effects in carrier-based sensorless control of PM synchronous machines," IEEE Trans. Ind. Appl., Vol. 46 (1), pp. 139–149, Jan./Feb. 2010.

[11] D. Raca, P. García, D. Reigosa, F. Briz, and R.D. Lorenz, "Carrier Signal Selection for Sensorless Control of PM Synchronous Machines at Very Low and Zero Speeds," IEEE Trans. Ind. Appl., Vol. 46 (1), pp. 167–178, Jan./Feb. 2010.

[12] Y. Yoon, S. Sul, S. Morimoto and K. Ide, "High Bandwidth Sensorless Algorithm for AC Machines Based on Square-wave Type Voltage Injection," IEEE Trans. Ind. Appl., Vol. 47 (3), pp. 1361–1379, May/June 2011.

[13] L. Xu, E. Inoa, Y Liu and B. Guan, "A New High Frequency Injection Method for Sensorless Control of Doubly-Fed Induction Machines," IEEE Trans. Ind. Appl., Vol. 48 (5), pp. 1556–1565, Sept./Oct. 2012.

[14] B. Shen, B. Mwinyiwiwa, Y Chang and B.T. Ooi "Sensorless Maximum Power Point Tracking of Wind by DFIG Using Rotor Position Phase Lock Loop (PLL)", IEEE Trans. Power Elect., vol. 24 (4), pp. 942-951, Apr. 2009.

[15] R. Cardenas, R. Peña, J. Proboste, G. Asher and J. Clare, "MRAS Observer for Sensorless Control of Standalone Doubly Fed Induction Generators", IEEE Trans. Energy Conv., vol. 20 (4), pp. 710-718, Dec. 2005.

[16] S. Yang and Venkataramana Ajjarapu, "A Speed-Adaptive Reduced-Order Observer for Sensorless Vector Control of Doubly Fed Induction Generator-Based Variable-Speed Wind Turbines", IEEE Trans. Energy Conv., vol. 25 (3), pp. 891-900, Sept. 2010.

[17] A. Rambetius and B. Piepenbreier, "Carrier signal based sensorless control of wound field synchronous machines using the rotor winding as the receiver: Rotating vs. alternating carrier," PCIM Europe Conference, pp. 293–300, May 2015.

[18] A. Rambetius and B. Piepenbreier, "Sensorless control of wound rotor synchronous machines using the switching of the rotor chopper as a carrier signal," IEEE SLED, pp. 1–8, Oct. 2013.

[19] A. Rambetius and B. Piepenbreier, "Comparison of carrier signal based approaches for sensorless wound rotor synchronous machines, " IEEE SPEEDAM , pp. 1142-1159, 2014

[20] D. Uzel, V. Smidl and Z. Peroutka, "Estimator comparison for Resolver Motivated Sensorless Rotor Position Estimation of Wound Rotor Synchronous Motors, " IEEE EPE, pp. 26-28 Aug. 2014.

[21] D. Reigosa, J. M. Guerrero, A. B. Diez and F. Briz, "Rotor Temperature Estimation in Doubly-Fed Induction Machines Using Rotating High Frequency Signal Injection, " IEEE Trans. Ind. Appl., Vol. 53 (4), pp. 3652 - 3662, March 2017.

[22] D. Reigosa, D. Fernandez, H. Yoshida, T. Kato and F. Briz, "Permanent magnet temperature estimation in PMSMs using pulsating high frequency current injection", IEEE Trans. on Ind. Appl., 51(4): 3159-3168, Jul./Aug. 2015.

[23] D. W. Novotny and T. A. Lipo, "Vector Control and Dynamics of AC Drives," Oxford Science Publications, 1996.

[24] D. Reigosa, D. Fernández, M. Martinez, J. M. Guerrero, A. B. Diez, F. Briz, "Magnet Temperature Estimation in Permanent Magnet Synchronous Machines Using the High Frequency Inductance", IEEE Trans. on Ind. Appl., 55(3): 2750- 2757 May/June 2019. DOI: 10.1109/TIA.2019.2895557

[25] Analysis of Magnet Thermal and Magnetization State Monitoring in PMSMs Based on High Frequency Signal Injection" IEEE Trans. on Ind. Appl., accepted: publication pending, 2020. DOI: 10.1109/TIA.2019.2952027.

[26] H. Han, T. M. Jahns, and Z. Q. Zhu, "Analysis of rotor core eddy- current losses in interior permanent magnet synchronous machines," *IEEE IAS*, pp- 1-8, Oct. 2008,.

[27] K. Atallah, D. Howe, and D. Stone, "Rotor loss in permanent-magnet brushless AC machines," *IEEE Trans. Ind. Appl.*, vol. 36, no. 6, pp. 1612–1618, Nov./Dec. 2000.

[28] D. Reigosa,D. Fernandez , C. Gonzalez, S. B. Lee and Fernando Briz "Permanent Magnet Synchronous Machine Drive Control using Analog Hall-Effect Sensors" IEEE Trans. on Ind. Appl., 54(3): 2358-2369, May/June 2018.